buildings

MDPI

Article

Influence of Pile Spacing on the Compressive Bearing Performance of CEP Groups

Yongmei Qian [1,*], Qingzhi Cao [1], Yang Yang [2], Da Teng [3] and Tingting Zhou [4]

[1] College of Civil Engineering, Jilin Jianzhu University, Changchun 130118, China; 18168131268@163.com
[2] Jilin College of Architecture Science and Technology, Changchun 130114, China; 13843045833@163.com
[3] Changchun Institute of Architecture, Changchun 130604, China; 15318731115@163.com
[4] Jilin Construction Engineering Group Co., Ltd., Changchun 130051, China; 19917271725@163.com
* Correspondence: qianyongmei@jlju.edu.cn

Abstract: Pile spacing is an important factor affecting the bearing capacity of concrete expansion pile (CEP) groups. In this study, a pile group was simulated and analyzed using ANSYS software R19.0. The influence of pile spacing on the bearing capacity of the pile group under a vertical load was determined using three sets of four-, six-, and nine-pile models with different pile spacings. The grid division of the pile soil model adopts a mapping method, using the contact types of rigid and flexible bodies and applying surface loads to the model piles step-by-step. After vertical pressure was applied to the model pile, in-depth analysis was conducted on the displacement cloud map, pile top displacement, and other data. The different stress conditions of corner, edge, and center piles in each model group were compared and analyzed, revealing the relationship between the stress mechanism and failure law of the soil around the pile and the pile spacing. It was found that the soil displacement range of edge piles is slightly larger than that of corner piles. This phenomenon gradually decreases with increasing pile spacing. When the pile spacing increases to four times the cantilever diameter, the difference in soil displacement at different pile positions is small, and the pile spacing has little effect on the compressive bearing capacity of the pile group. Thus, it is reasonable to control the pile spacing at three to four times the cantilever diameter. In the nine-pile model, when the load is loaded to the 20-step level, the displacement value of the central pile is −72.278 mm, while the displacement values of the edge pile and corner pile are −69.012 mm and −66.806 mm. It is shown that increasing the pile spacing can effectively reduce the pile group effect and improve the bearing capacity of the pile foundation. At present, CEP pile groups are gradually being applied in practical engineering, but research on the influence of pile spacing on the compressive bearing performance of CEP pile groups is still at a very early stage. This article reinforces the influence of pile spacing on the compressive bearing performance of CEP pile groups. It provides theoretical support for its application in practical engineering.

Keywords: concrete expansion pile (CEP) group; ANSYS finite-element simulation; pile spacing; different pile positions; compression bearing performance

check for updates

Citation: Qian, Y.; Cao, Q.; Yang, Y.; Teng, D.; Zhou, T. Influence of Pile Spacing on the Compressive Bearing Performance of CEP Groups. *Buildings* **2024**, *14*, 1447. https://doi.org/10.3390/buildings14051447

Academic Editors: Eugeniusz Koda and Wusheng Zhao

Received: 1 April 2024
Revised: 9 May 2024
Accepted: 11 May 2024
Published: 16 May 2024

1. Introduction

With the rapid development of urban high-rise buildings, pile foundations, an economical form of foundation, are being widely used in engineering. They are mainly composed of a large number of piles and caps buried in the foundation. The function of a pile foundation is to transfer the load to the soil layer deep underground, which satisfies the requirements of the building foundation for bearing capacity and settlement [1,2]. The pile in the pile foundation is a type of force transmission component that has strong stiffness and bending resistance, and it is the focus of high-rise building foundation construction. For heavy structures, weak soils have to be improved before the construction work occurs. One of the methods used for stabilizing soils is the deep mixing pile [3,4]. Moreover, a new type of variable cross-section concrete cast-in-place pile, called CEP, has been used to sustain such heavy structures. With increase in the number of building floors, the load on the foundation bottom also increases, making it particularly important to choose a safe, efficient, and economical type of pile body [5].

CEPs are a new type of variable cross-section concrete cast-in-place pile that has advantages such as high bearing capacity, small settlement, energy conservation, and environmental protection [6–9]. An engineering diagram of a CEP is shown in Figure 1. Some results on the compressive bearing performance of single and double CEPs have been obtained through research [10,11]. In practical engineering, CEP pile groups are widely used [8,12]. The spacing between the piles is an important factor that affects the failure mechanism and bearing capacity of CEP groups. Reducing the spacing between piles can reduce foundation settlement. However, the load borne by the piles is excessively large, making it difficult to fully utilize the bearing potential of the soil between the piles. Increasing the spacing between piles may not meet the requirements of bearing and deformation and can easily cause excessive stress concentration at the pile top [9,13]. Therefore, it is necessary to determine a reasonable spacing between piles to reduce costs, shorten the construction period, and improve engineering quality. Therefore, it is necessary to conduct in-depth research on the relationship between the bearing capacity of CEP groups and variations in pile spacing.

Figure 1. Drawing of CEP.

Prior to this study, large-scale pile soil solid tests and a large number of laboratory small model tests were conducted at a construction site [14]. The laboratory small model tests mainly used a reaction loading platform device as shown in Figure 2. The reaction loading platform primarily comprised a reaction beam, a pull-out instrument, and a displacement sensor, which uses the reaction beam to apply downward pressure. When the experimental and ANSYS simulation data were compared and analyzed, the results were basically consistent, confirming the accuracy of using ANSYS software to simulate and analyze the data in this study in order to examine the compressive bearing performance of CEP groups. A mapping method was used for grid division of the pile soil model, and the contact type required between the rigid and flexible bodies was identified. Grid refinement was applied to the bearing plate, though grid refinement was not required for the less affected pile body and pile soil [15–17]. Vertical surface loads were gradually applied to the model piles. The pile spacing was selected as the sole variable, and graded loading was applied to three different pile spacing (two to four times the overhanging diameter) models under four-, six-, and nine-pile situations [18]. The top displacement of each stage of the pile and the failure state of the soil around the pile were recorded using ANSYS software under a vertical load, and relevant displacement cloud maps were extracted to analyze the bearing performance of the pile, the changes in the soil around the pile, and the pile–soil effect under different pile spacings [19]. A comparative analysis of the stress conditions of corner, edge, and center piles was conducted. The research results obtained fill the gap in the literature on the compressive capacity of CEP pile groups. They provide a theoretical basis for the practical application of CEP groups in engineering.

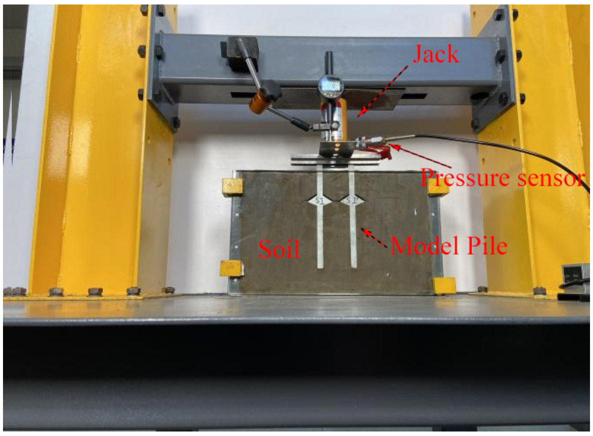

Figure 2. Compression test of double piles.

2. ANSYS Finite-Element Modeling

2.1. Material Parameters

The soil was made of powdery clay and the CEP body was composed of C30 concrete with a pile–soil friction coefficient of 0.3 [20]. The parameters of the pile body and soil are listed in Table 1.

Table 1. Pile–soil parameters.

Materials	Density (kg/m^3)	Elastic Modulus (MPa)	Poisson's Ratio	Cohesion (MPa)	Friction Angle (°)	Expansion Angle (°)	Pile–Soil Friction Coefficient
Concrete	2.25×10^3	3.0×10^4	0.2	--	--	--	0.3
Clay	1.688×10^3	40	0.35	0.04355	10.7	10.7	

2.2. Model Parameters

Based on previous research results on single and double CEPs, the CEPs were modeled in a 1:1 ratio. The model parameters are as follows: pile length of 10,000 mm, pile diameter of 500 mm, and slope corner on the plate α taking a 45° downward slope and corner β taking a 27° one, with the overhang length of plate being 500 mm. The load-bearing plate is set at a distance of 3.5 m from the top of the pile. A schematic diagram of the model is shown in Figure 3. In the case of four piles, the spacing between the piles was selected to be two, three, and four times the overhang length of plate for this research (S2, S3, and S4, respectively). In the case of six piles, the spacing between the piles was selected to be two, three, and four times the overhang length of plate for this research (L2, L3, and L4, respectively). Owing to the significant difference in the overall dimensions between the front and side in the case of six piles, a set of different spacings between the front and side piles was added for comparison. Specifically, the distance between Piles 1, 2, and 3 was three times the overhang length of plate, and the distance between Piles 1 and 4 was four times the overhang length of plate, designated as L3+4. For the nine piles, the pile spacing was selected to be two, three, and four times the overhang length of plate (J2, J3, and J4, respectively). The layout plans for four, six, and nine piles are shown in Figure 4.

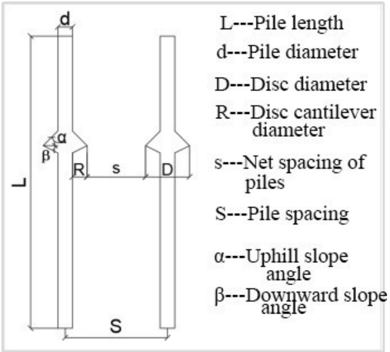

Figure 3. Schematic diagram of model pile.

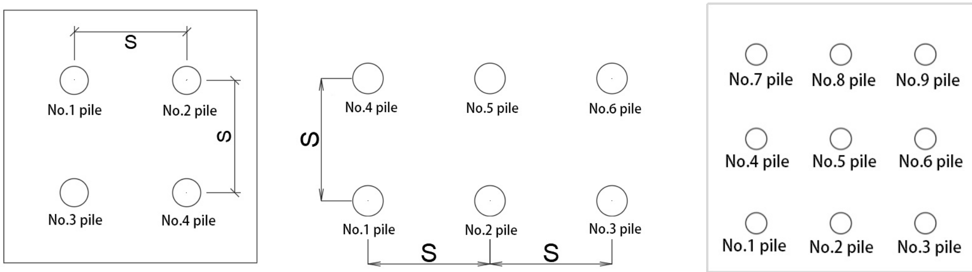

Figure 4. Layout plan of four piles, six piles, and nine piles.

2.3. Model Construction Process and Loading Plan

CEPs were modeled based on the data of the pile body. This simulation studies the soil around the pile as a single soil layer, using the Drucker–Prager function model. The material properties of the pile body are set to linear elasticity, the pile body is set to Solid 65 to simulate actual concrete parameters, and the soil is set to Solid 45 to simulate actual silty clay parameters. The Solid 45 entity unit has eight nodes, each with translational degrees of freedom along the X-, Y-, and Z-directions. Distributed loads can be applied on all sides of the unit. The model can be applied to solving problems related to large displacement, large strain, plasticity, and yield analysis. The output results of the Solid 45 element solution include node displacement, principal stress, normal stress, shear stress, and total strain in all directions. The Solid 65 solid elements are specifically developed on the basis of Solid 45 to establish finite element models for problems with reinforced concrete or concrete materials. To ensure the calculation accuracy of the simulation analysis, the load-bearing plate area will be locally refined with mesh refinement. The elastic modulus of the pile is much greater than that of the soil, so the contact mode of the pile–soil model is set as rigid flexible contact. The rigid surface of the pile is set as the target surface and the geometric shape and material characteristics of the pile are described using target170 elements. It is a nonlinear, bending stiffness distributed pile element suitable for simulating the deformation and stress distribution of piles. The contact173 element is used to describe the frictional force and contact pressure between the pile soil contact surfaces. This unit can consider the non-linear characteristics of the contact surface, including frictional slip, normal stiffness, and changes in the contact area. The load applied in this study was a vertical load, so the top of the soil model was not constrained by the Y-direction degrees of freedom, while the other five degrees of freedom in the X-, Y-, and Z-directions were all constrained. Using a step-by-step loading method, 100 kN was loaded onto the top of each pile at each step. Ten groups of pile group models were loaded in stages for four, six, and nine piles. The loading was terminated when the simulation analysis curve did not converge and was considered to have reached the ultimate load.

3. Analysis of ANSYS Finite-Element Simulation Results

3.1. Displacement Cloud Map

3.1.1. Four-Pile Displacement Cloud Map

The four-pile model extracted displacement cloud maps corresponding to three sets of model piles under an applied load of 8800 kN as a reference, as shown in Figure 5.

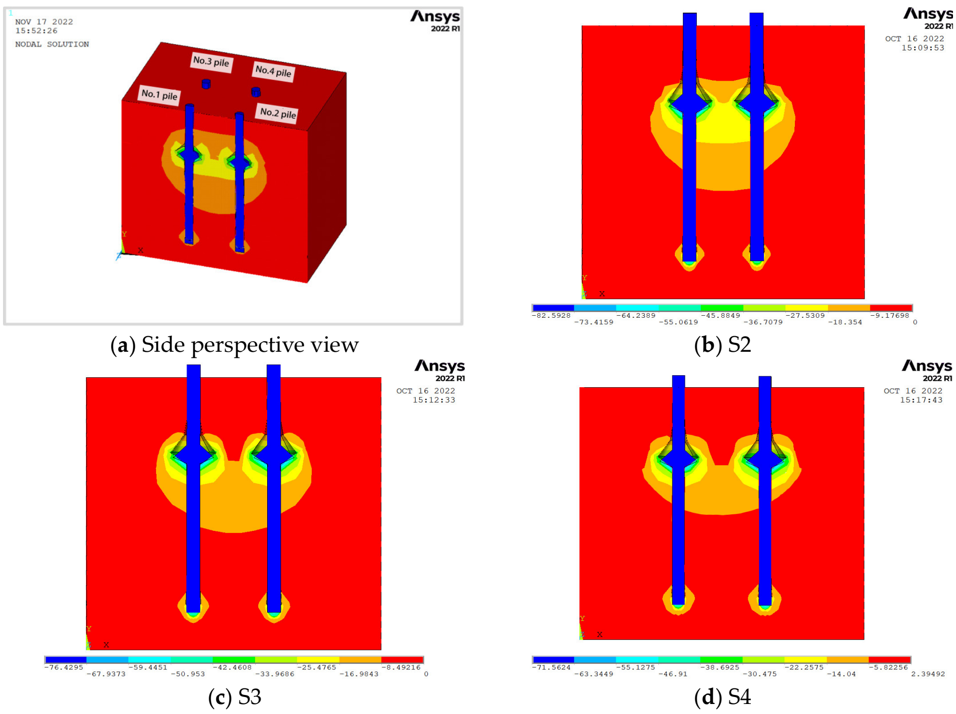

Figure 5. Perspective view and displacement cloud map of the displacement side under the same load from S2 to S4.

(1) The overall trends in the displacement cloud maps for the three sets of model piles are basically consistent. Under vertical pressure, the soil below the bearing plate of the four-pile body is compressed, resulting in different degrees of sliding and displacement. The area with a higher pressure corresponds to a greater downward displacement, and the displacement of the soil outside the pile is significantly smaller than that on the inside. Therefore, there is soil interaction on the inside of the pile under the bearing plate as the center, and the main damage range of the soil is in the area near the bearing plate with high vertical pressure (green area in the figure). As the distance between the piles increases, the damage range and displacement cloud map of the soil around the piles also change.

(2) In Figure 5b,c, the spacing between these two groups of piles is relatively small: 2000 and 2500 mm, respectively (with a net spacing of one and two times the overhang length of the plate). In these two groups, there is a significant displacement overlap (green area) in the soil below the bearing plates of the adjacent piles. This is because of the soil superposition effect caused by the close arrangement of the piles, which leads to a decrease in the bearing capacity of the soil between the piles. There is a significant overall downward displacement of the soil inside the pile.

(3) As shown in Figure 5d, when the spacing between piles increases to 3000 mm (the net spacing between piles is three times the overhanging diameter of the plate), the weight of the soil under the plate is relatively small when the two adjacent piles reach failure, and only a small part of the soil undergoes a small displacement overlap. At this time, the pile group effect is smaller than that in Figure 5b,c, indicating that, as the spacing between piles increases, the pile–soil effect gradually decreases. Furthermore,

comparing the displacement of the coordinate axis reveals that the carrying capacity constantly increases.

3.1.2. Six-Pile Displacement Cloud Map

The displacement cloud map of the front row piles of the six-pile model under ultimate load was extracted for comparative analysis, as shown in Figure 6.

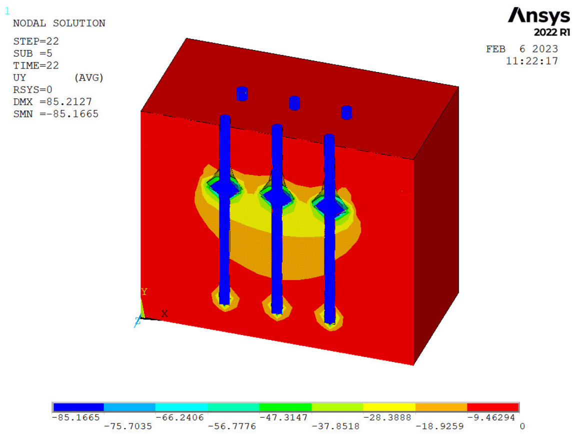

(**a**) L2

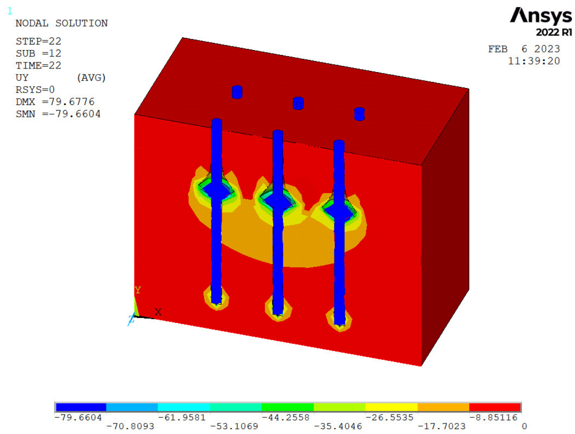

(**b**) L3

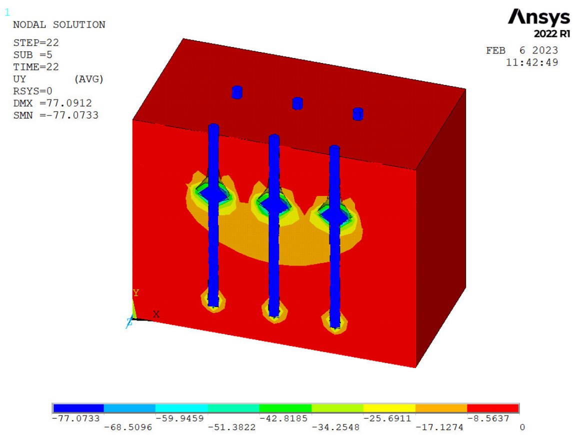

(**c**) L3+4

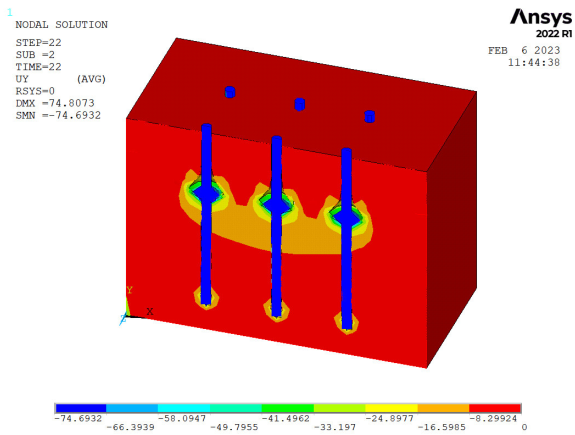

(**d**) L4

Figure 6. Cloud diagram of displacement for each group under ultimate load of L2–L4.

The displacement cloud map of the four pile spacing groups under the ultimate load is basically similar; however, as the pile spacing increases, the influence range of the soil under the ultimate load gradually decreases, indicating that the stress state and bearing performance of the six piles are basically consistent with those of the four piles, which is in line with the working mechanism of the group piles and can be further analyzed. Comparing the displacement cloud maps of the four front-row pile profiles reveals that the displacement range of the soil on both sides of the piles is significantly smaller than that of the soil on the middle pile, and this phenomenon gradually decreases with an increase in pile spacing. Comparing the displacement cloud maps of the L3 and L3+4 groups shows that, for the six piles, the arrangement of the L3+4 group is more reasonable, indicating that increasing the distance between adjacent piles on the side can improve their bearing capacity. In pile groups, the bearing capacity varies depending on the location of the piles. For intermediate piles, the size of their bearing capacity increases with an increase in pile spacing, further confirming that the soil effect of the piles in the group on the overall bearing performance cannot be ignored.

3.1.3. Nine-Pile Displacement Cloud Map

In the nine-pile model, the displacement contours of the front and second rows of piles were extracted for comparison and analysis of each group of piles under the 20-step load conditions, as shown in Figure 7.

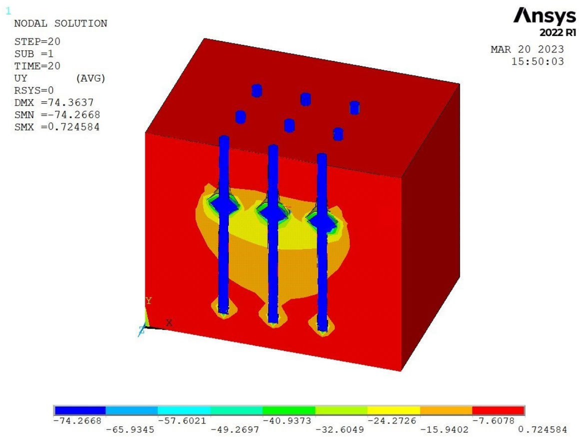

(**a**) J2 Front Row

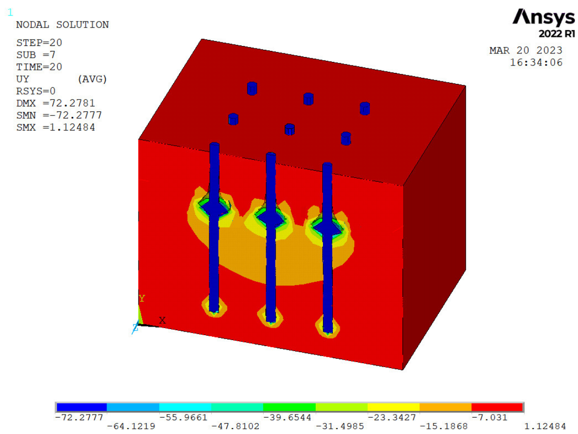

(**b**) J3 Front Row

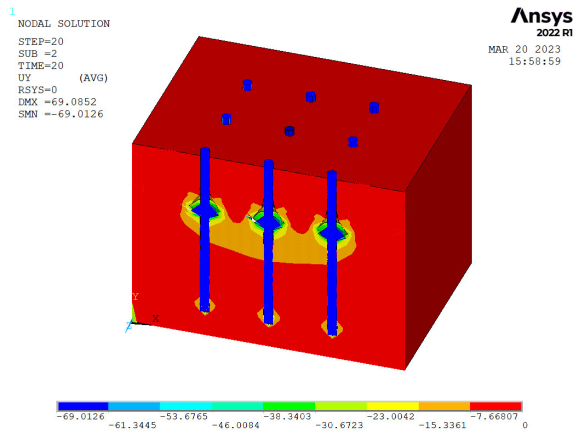

(**c**) J4 Front Row

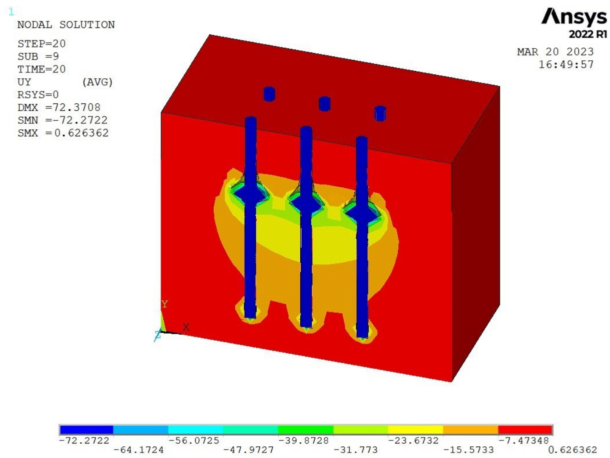

(**d**) J2 Middle Row

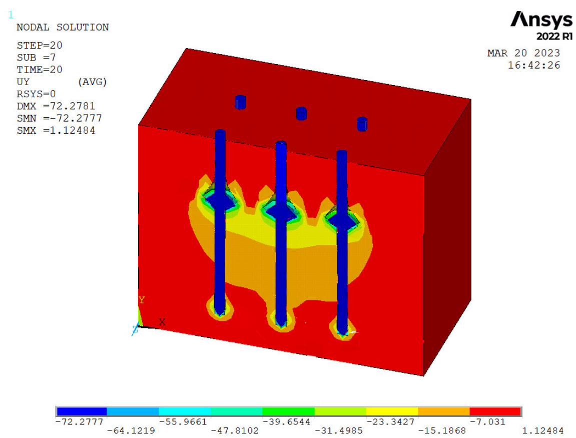

(**e**) J3 Middle Row

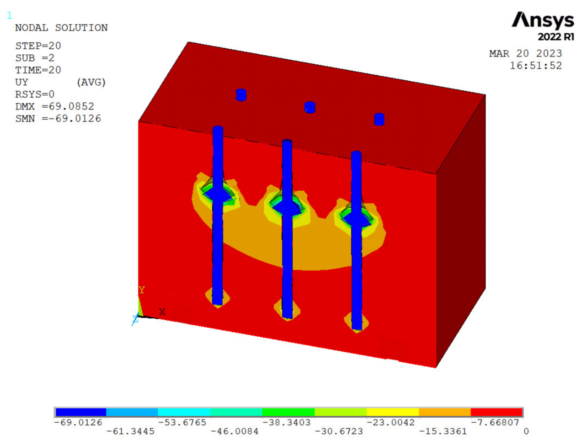

(**f**) J4 Middle Row

Figure 7. Displacement cloud maps of different sections under different pile spacings.

(1) Under the same load, the displacement cloud maps of the front and middle rows of the three pile spacing groups are basically consistent. As the pile spacing increases, the

influence range of the soil around the pile gradually decreases, which is consistent with the mechanism of pile group action.

(2) Comparing the displacement cloud maps of the front and middle rows of piles, when the pile spacing is the same, the soil influence range of the profile map of the front row of piles is significantly smaller than that of the middle row of piles, and the displacement range of the soil around the piles gradually decreases from inside to outside. This indicates that the soil overlap range between the center pile and adjacent piles is larger than that between the edge and corner piles, resulting in a slightly smaller bearing capacity of the soil around the middle pile than that of the edge and corner piles. (3) The corner piles (Pile 1) and edge piles (Pile 4) of each group show that the soil displacement range of the edge piles is slightly larger than that of the corner piles, and this phenomenon gradually decreases with an increase in pile spacing. When the pile spacing increases to four times the cantilever diameter of the plate, the displacement difference between the corner, edge, and center piles is small and can be ignored. Therefore, when limited by the site, it is more reasonable to control the pile spacing by three to four times when the plate is suspended.

3.2. Comparative Analysis of Pile Displacement

3.2.1. Comparative Analysis of Corner and Edge Piles under Six-Pile Conditions

For six piles, four sets of simulated displacement values of the corner and edge piles were extracted under the ultimate load, and displacement curves were drawn, as shown in Figure 8.

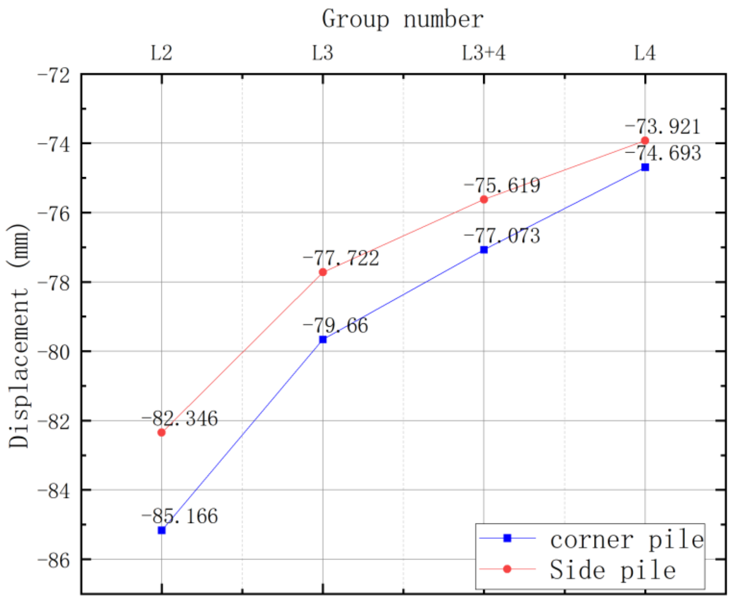

Figure 8. Displacement of corner and edge piles under ultimate load.

Owing to the different positions of each of the six piles, there are certain differences in their displacement values under the ultimate load. The displacement value of the corner pile is significantly greater than that of the edge pile. And as the spacing between piles increases, the difference in displacement values between edge piles and corner piles gradually decreases. The displacement value of the pile top of the L2 group of edge piles with smaller pile spacing decreases by 3.31% compared with the displacement value of the pile top of the edge pile. The displacement value of the L4 group corner piles with larger pile spacing decreases by 1.03% compared with the displacement value of the edge piles. This phenomenon indicates that, when the pile spacing is small, the shared range of the soil around the pile body is larger. The main reason is that the increase in pile spacing gradually reduces the pile–soil effect, increases the range of soil that can provide bearing capacity, and increases the bearing capacity of the soil around the edge piles. Based on the displacement cloud map in Figure 3, it can be concluded that an increase in pile spacing reduces the mutual influence between adjacent piles while reducing the group pile effect and improving the bearing capacity.

To study the effects of different pile spacings on the bearing performance of the six piles during the loading process, the displacement data of the pile top load for each group of edge piles with the highest displacement under each load level were extracted, and the load–displacement curve was plotted, as shown in Figure 9. The load–displacement data are shown in Table 2.

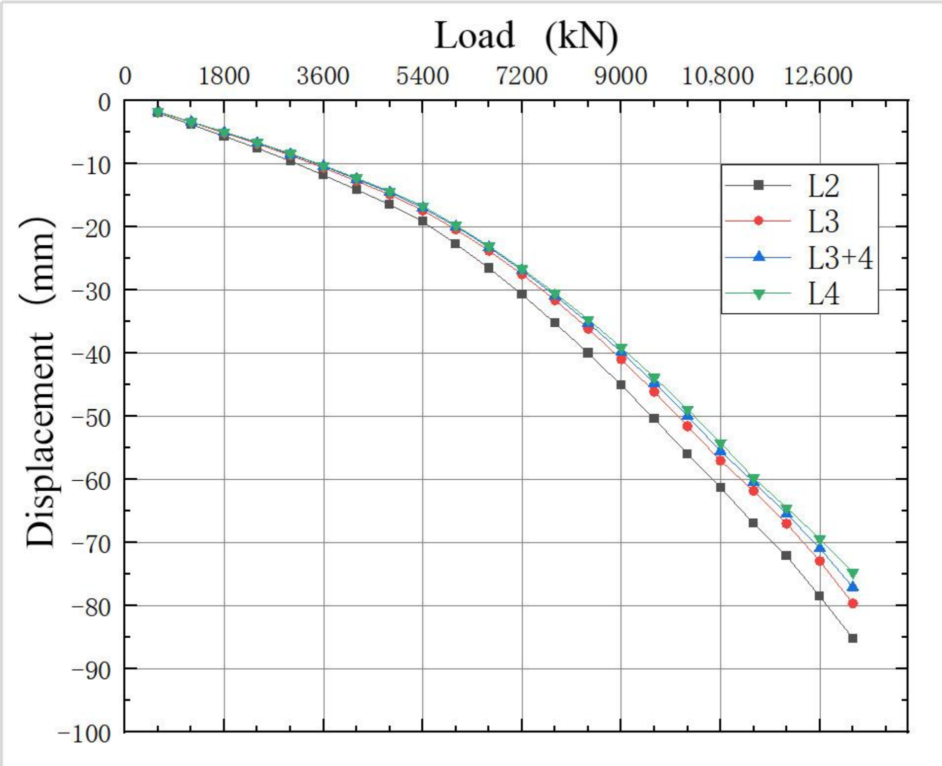

Figure 9. Load–displacement data curves of six piles under different loads.

Table 2. Displacement data table of the edge pile top under different loads of the six piles.

Load (kN)	Displacement (mm)			
	L2	L3	L3+4	L4
600	−1.896	−1.714	−1.677	−1.669
1200	−3.764	−3.405	−3.330	−3.313
1800	−5.610	−5.076	−4.964	−4.935
2400	−7.485	−6.787	−6.636	−6.573
3000	−9.542	−8.636	−8.436	−8.356
3600	−11.758	−10.625	−10.370	−10.244
4200	−14.054	−12.696	−12.392	−12.233
4800	−16.431	−14.859	−14.500	−14.334
5400	−19.095	−17.332	−16.954	−16.680
6000	−22.654	−20.335	−19.883	−19.710
6600	−26.505	−23.735	−23.201	−23.039

Table 2. *Cont.*

Load (kN)	Displacement (mm)			
	L2	L3	L3+4	L4
7200	−30.675	−27.473	−26.842	−26.625
7800	−35.238	−31.583	−30.832	−30.468
8400	−39.962	−36.115	−35.186	−34.636
9000	−45.070	−40.942	−39.807	−39.084
9600	−50.401	−46.090	−44.715	−43.840
10,200	−55.965	−51.546	−49.957	−48.874
10,800	−61.270	−57.005	−55.508	−54.201
11,400	−66.979	−61.804	−60.393	−59.746
12,000	−72.141	−66.995	−65.449	−64.474
12,600	−78.518	−72.926	−70.920	−69.375
13,200	−85.166	−79.660	−77.073	−74.693

(1) During the entire loading stage, the displacement of each group of piles decreases with increase in pile spacing. The displacement values of L4 and L2 groups when reaching the ultimate load were compared. The displacement of the pile top decreases from 85.166 to 74.693 mm, and the settlement of the pile top decreases by 12.3%, indicating that increasing the pile spacing can improve the bearing capacity of the pile group. Comparing the displacement curves of the L3 and L3+4 groups reveals that the trends of the two load–displacement curves are consistent. The pile top displacement value of the L3+4 group is slightly smaller than that of the L3 group, and the pile top displacement value of the L3+4 group is reduced by 3.25% compared with that of the L3 group. This indicates that increasing the distance between the piles on the side with fewer piles can improve the bearing capacity when the number of asymmetric piles is on the front and side. This is mainly due to the stress superposition phenomenon of the soil under the bearing plate under the vertical load. As the spacing between adjacent piles increases, the soil effect gradually decreases. Thus, the optimal pile spacing can reduce the settlement of pile groups.

(2) The load–displacement curve shows that the loading process is roughly divided into two stages. With 6000 kN as the boundary point, the curve tends to flatten before 6000 kN, indicating that, in the early stage of loading, most of the load is borne by the pile side friction and the soil at the pile end. At this time, the soil below the bearing plate remains in a compressed state and has not fully played its role. When the load exceeds 6000 kN, the slope of the curve increases; however, there is no sharp drop, indicating that the overall performance of the pile group is good. At this point, the lateral frictional resistance can no longer bear the load; at the same time, the bearing plate begins to take effect. The load on the pile top spreads to the soil through the bearing plate, thereby reducing the settlement of the pile group.

3.2.2. Comparative Analysis of Displacement at the Tops of Corner, Edge, and Center Piles under the Condition of Nine Piles

In the case of nine piles, the pile top displacements of the representative J3 group corner, edge, and center piles (Piles 1, 2, and 5 in Figure 4) at asynchronous levels were extracted, and a curve graph was drawn, as shown in Figure 10.

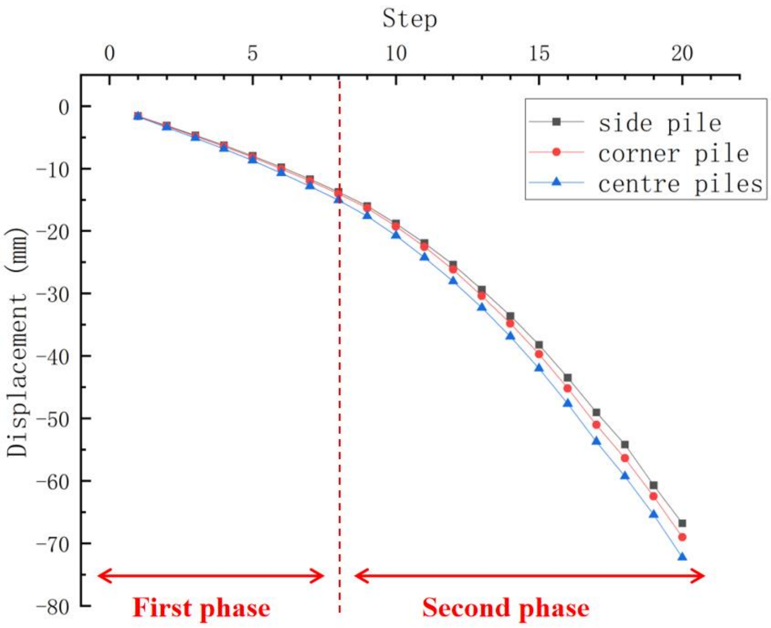

Figure 10. Pile top displacements at different positions under each step.

Under the same load, the displacements of the piles vary depending on their positions. The loading process can be roughly divided into two stages. In the first stage, the three curves basically overlap, and the displacement values of the three piles have little difference. This indicates that, when the load is small, the soil under the plate has a stronger load-bearing capacity, and the trends of the changes in the soil around the piles at different positions are basically the same. In the second stage, the degree of separation of the three curves is significantly greater than that in the first stage, and the load on the central pile gradually exceeds that on the edge and corner piles. After loading to the 20-step level, the displacement value of the center pile is −72.278 mm, and the displacement values of the edge and corner piles are −69.012 and −66.806 mm, respectively. Compared with the center pile, their displacement values are reduced by 4.52% and 7.57%, respectively. Overall, when subjected to vertical pressure, due to the overlapping parts of the soil between piles, the displacement value generated by the central pile is the largest, followed by the edge pile and corner pile, and the difference also increases with the increase in load.

3.2.3. Analysis of Displacement at the Top of the Central Pile under the Condition of Nine Piles

The center pile with the largest displacement among the nine piles was considered as the research object. The displacement curves of the pile top under different loads were plotted, as shown in Figure 11.

(1) The trend of load displacement data curves for nine and six piles is basically the same. The ultimate load values of six and nine piles were 13,200 kN and 18,000 kN, respectively, which increased by 36.3%. The main reason is that with increase in the number of piles, the load shared by each pile decreases, and the settlement of the pile group also decreases. However, increasing the number of foundation piles requires attention to adaptability. Otherwise, increasing the number of foundation piles will expand the range of stress superposition between different piles, affecting the full play of the pile side and pile end resistance. Moreover, an excessive number of foundation piles will increase costs and have low cost-effectiveness.

(2) Throughout the loading phase, the trends in the load–displacement data curves for J2, J3, and J4 are basically the same. The displacement of each group of piles decreases with an increase in pile spacing. After loading to the ultimate load, the displacement of the pile top decreases from 74.267 to 69.012 mm, and the settlement of the pile top decreases by

7.6%. Compared to the settlement variation under the six-pile situation, the displacement value of the pile top of the nine piles is slightly smaller than that of the six piles. The main reason is that when the nine piles are arranged, the overlap range of the soil between the piles increases, and the group pile effect is obvious.

(3) At the initial stage of loading, the settlements at the tops of piles with different spacings are basically the same; however, as the load gradually increases, the settlements of the three groups of piles begin to show significant differences. When the pile top load is constant, with an increase in pile spacing, the degree of separation between the J2 and J3 curves is significantly greater than that between J3 and J4, indicating that the larger the pile spacing, the smaller the pile group effect, and the higher the bearing capacity.

(4) During the entire loading stage, the settlement value of the pile group at the top of the pile decreases with increasing pile spacing. The load–displacement curve shows that, when the pile spacing is three and four times the overhang length of the plate, the distance between the two curves is extremely small, indicating that the increase in the pile top displacement of J4 compared with J3 is extremely small. Continuing to increase the pile spacing does not have a significant effect on reducing settlement. In addition, the larger the pile spacing, the greater the construction difficulty, which is not conducive to practical application. Therefore, it is reasonable to control the pile spacing at three to four times the overhang length of the plate.

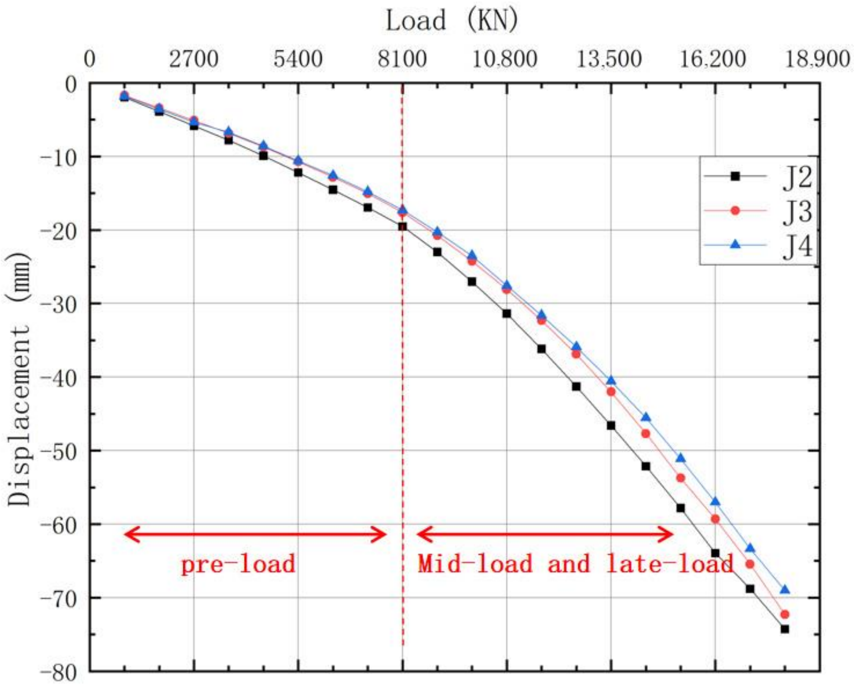

Figure 11. Load displacement data curves of pile top under different loads.

3.3. Comparative Analysis of Soil Displacement on Both Sides of the Edge and Center Piles under Six-Pile Condition

The displacement values corresponding to each node of the six piles under the ultimate load were extracted, the node was selected, as shown in Figure 12a, and three groups of curves were drawn according to the displacement value of the soil node on each side, as shown in Figure 12b–d.

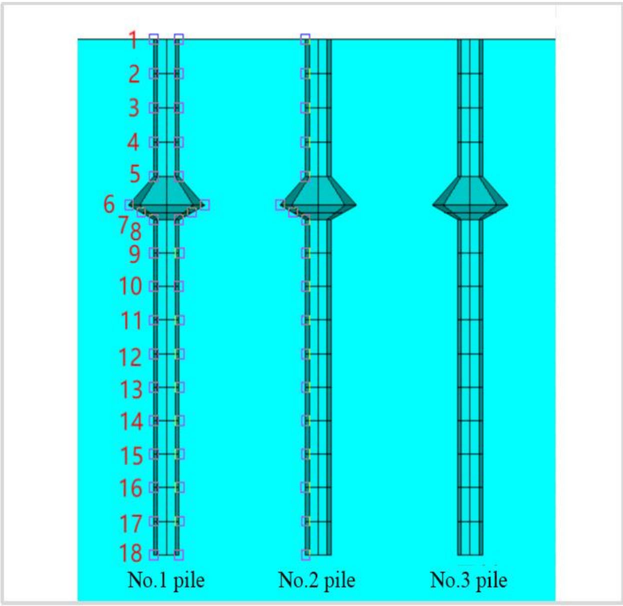

(**a**) Node selection

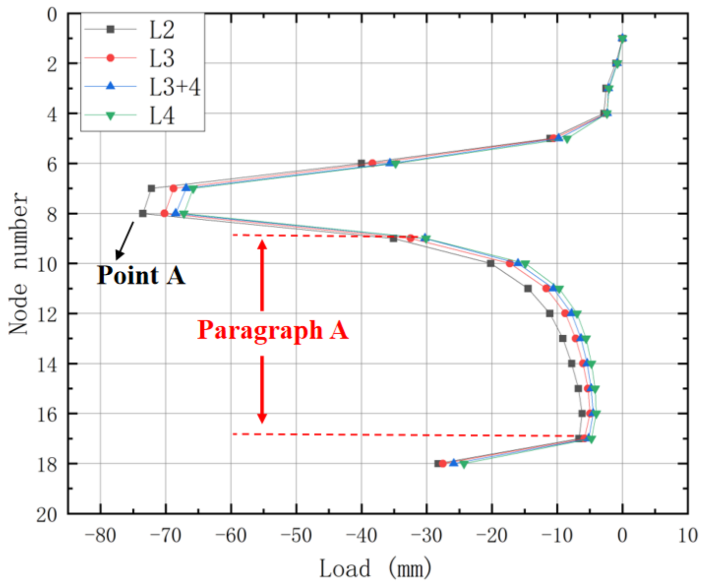

(**b**) Left soil displacement of Pile 1

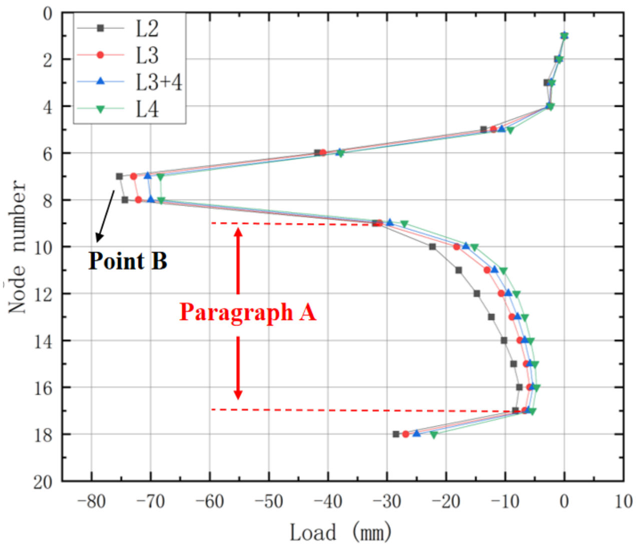

(**c**) Displacement of soil on the right side of Pile 1

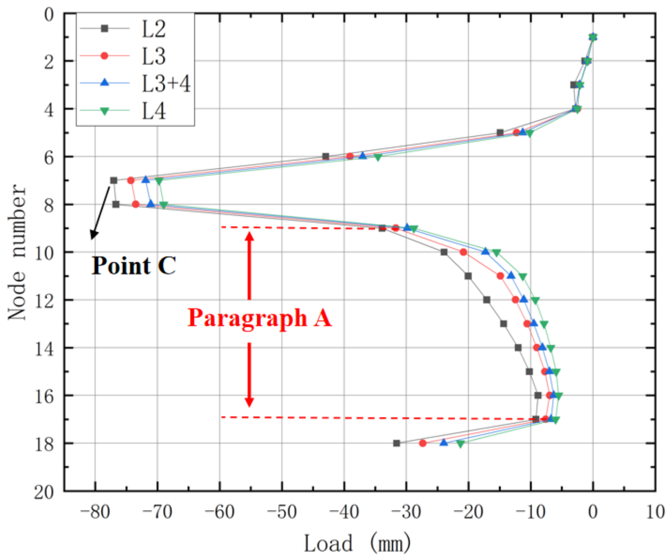

(**d**) Left soil displacement of Pile 2

Figure 12. Soil displacements at different positions under ultimate load of L2–L4.

(1) The displacement values of the three sets of curve graphs show a trend of increasing from small to large and then decreasing, and all undergo sudden changes at the bearing plate. The maximum displacement occurs at the lower part of the bearing plate, followed by the pile end. The reason is that under vertical pressure, the bearing plate bears most of the load, while the pile end and lateral friction share a small amount of the load.

(2) The maximum displacement of the soil on the left side of Pile 1 in Figure 12b is at Node 8 of Group L2 (Point A in the figure), with a displacement value of −73.51 mm. The corresponding displacement values of the other three groups of Node 8 are −70.19, −68.51, and −67.23 mm. The maximum displacements of the soil in Groups L3, L3+4, and L4 decrease by 4.52%, 6.8%, and 8.54%, respectively, compared with the maximum displacement of Group L2. Similarly, on the right side of Pile 1 and left side of Pile 2, the maximum displacement is at Node 7 (Points B and C in the figure). Node 7 is located at the midpoint below the plate, with the displacement values at Points B and C being −75.31 and

−77.02 mm, respectively. As shown in Figure 12c, the maximum displacements of the other three groups relative to Point B decrease by 3.19%, 6.37%, and 9.23%, respectively. Similarly, as shown in Figure 12d, the maximum displacements of the other three groups relative to Point B decrease by 3.6%, 6.65%, and 9.47%, respectively. Comparing the soil displacements on the side of the pile at three different positions reveals that the displacement of the soil on the inner side of the pile is slightly greater than that on the outer side. The reason is that because of the compression of the soil between piles and the effect of pile groups, the displacement of the soil in the inner side of the pile body will be slightly larger than that in the outer side. In practical engineering, it is possible to increase the spacing between the piles appropriately to reduce the soil effect on the inside of the piles. When the net spacing between the piles exceeds four times the overhang length of the plate, the improvement in the bearing capacity is negligible. At this time, it is not advisable to continue increasing the spacing between piles.

(3) Comparing the three sets of curve graphs, the displacement of Section A shows a significant change. The influence of pile spacing on the left soil displacement of Pile 1 is relatively small, whereas the influence on the left soil displacement of Pile 2 is significantly greater. The main reason is that the soil around Pile 2 is compressed by both Pile 1 and Pile 3, resulting in a decrease in the bearing capacity of the soil around Pile 2.

4. Conclusions

As a result of the finite-element simulation of the failure state of the soil around CEPs under vertical pressure with different pile spacings, the following conclusions are drawn:

(1) The trends in the displacement cloud maps for four, six, and nine piles are consistent. As the spacing between the piles increases, the range of influence of the soil around the piles gradually decreases.

(2) Furthermore, the soil displacement range of the edge pile is slightly larger than that of the corner pile, and this phenomenon gradually decreases with the increase in pile spacing. When the pile spacing increases to four times the overhang length of the plate, the difference in pile displacement at different positions is calculated to be extremely small and can be ignored. Therefore, the spacing between the piles should be controlled to be three to four times the overhang length of the plate, which is more reasonable.

(3) Under the same load, the displacement value of the central pile of the nine piles is −72.278 mm, while the displacement values of the edge pile and corner pile are −69.012 mm and −66.806 mm, respectively. Compared with the central pile, their displacement values have decreased by 4.52% and 7.57%, respectively. The displacement value generated by the central pile is the largest, followed by the edge and corner piles, and the difference increases with increasing load.

(4) When the pile spacing is small, the soil around the pile body shares a larger range. The smaller the pile spacing, the greater the impact on the edge and center piles. As the spacing between piles gradually increases, the mutual influence between adjacent piles gradually decreases, which not only reduces the pile group effect but also improves the bearing capacity.

Therefore, the spacing between piles will affect the bearing performance of pile groups. If engineering conditions permit, appropriate pile spacing should be selected to improve the bearing performance of the pile groups. In conclusion, this article contributes to improving the theoretical understanding of CEP piles in pile groups, providing a theoretical basis for practical engineering.

5. Discussion

This study used ANSYS software to simulate and analyze CEP pile groups and found that there were overlapping parts of the soil between the piles. During the arrangement of the pile groups, the overlapping range of the soil around the piles varied greatly depending on the location of the piles, resulting in different bearing capacities. Increasing the distance between piles can reduce the soil effect below the bearing plate of adjacent piles, and CEP pile groups have the best bearing performance when the distance between piles is controlled at three to four times the overhanging diameter of the plate. The results of this investigation fill the gap in the literature on the compressive capacity of CEP pile groups. However, in practical engineering, CEP pile groups are not only subjected to vertical forces but also horizontal and complex forces. The next step is to consider the impact of pile spacing on the load-bearing performance of pile groups under complex forces. Furthermore, the influence of other factors on the bearing performance of CEP pile groups, such as soil properties, plate position, number of plates, etc., requires to be considered in order to improve the theoretical understanding of CEP piles.

Author Contributions: Conceptualization, Y.Q. and Q.C.; methodology, Y.Q.; software, Q.C.; validation, Y.Y., D.T., and T.Z.; formal analysis, Y.Q.; investigation, Y.Q.; resources, Y.Q.; data curation, Y.Q.; writing—original draft preparation, Q.C.; writing—review and editing, Q.C.; visualization, Y.Q.; supervision, Y.Q.; project administration, Y.Q.; funding acquisition, Y.Q. All authors have read and agreed to the published version of the manuscript.

Funding: This research was funded by the National Natural Science Foundation of China under Grant number 52078239.

Data Availability Statement: Data are contained within the article.

Conflicts of Interest: Author Yang Yang was employed by Jilin College of Architecture Science and Technology. Author Da Teng was employed by Changchun Institute of Architecture. Author Tingting Zhou was employed by Jilin Construction Engineering Group Co., Ltd. The remaining authors declare that the research was conducted in the absence of any commercial or financial relationships that could be construed as a potential conflict of interest.

References

1. Chen, K. On the influence of pile foundation settlement of existing high-rise buildings on the surrounding buildings. *Adv. Civ. Eng.* **2021**, *2021*, 5560112. [CrossRef]
2. Do, D.H.; Pham, T.A. Investigation of performance of soil-cement pile in support of foundation systems for high-rise buildings. *Civ. Eng. J.* **2018**, *4*, 266. [CrossRef]
3. Odeh, N.A.; Al-Rkaby, A.H. Strength, Durability, and Microstructures characterization of sustainable geopolymer improved clayey soil. *Case Stud. Constr. Mater.* **2022**, *16*, e00988. [CrossRef]
4. Al-Rkaby, A.H.; Odeh, N.A.; Sabih, A.; Odah, H. Geotechnical characterization of sustainable geopolymer improved soil. *J. Mech. Behav. Mater.* **2022**, *31*, 484–491. [CrossRef]
5. Abdel-Azim, O.A.; Abdel-Rahman, K.; El-Mossallamy, Y.M. Numerical investigation of optimized piled raft foundation for high-rise building in Germany. *Innov. Infrastruct. Solut.* **2020**, *5*, 11. [CrossRef]
6. Gao, X.; Wang, J.; Zhu, X. Static load test and load transfer mechanism study of squeezed branch and plate pile in collapsible loess foundation. *J. Zhejiang Univ.-Sci. A* **2007**, *8*, 1110–1117. [CrossRef]
7. Ju, Y.; Chen, Y.F. Experimental study for the bearing capacity calculation of concrete expanded plates in squeezed branch piles. *Mater. Test.* **2018**, *60*, 1118–1124. [CrossRef]
8. Tang, S.T.; Chen, L.H. Field test of dx pile group. *Adv. Mater. Res.* **2011**, *243–249*, 2451–2455. [CrossRef]
9. Ma, H.; Wu, Y.; Tong, Y.; Jiang, X. Research on bearing theory of squeezed branch pile. *Adv. Civ. Eng.* **2020**, *2020*, 6637261. [CrossRef]
10. Qian, Y.; Li, X.; Ai, L.; Jiang, Y.; Dong, Y. Simulation Analysis of the Effect of Pile Spacing on the Compressive Load-Bearing Performance of CEP Double Piles. *Adv. Civ. Eng.* **2023**, *2023*, 1005985. [CrossRef]
11. Tian, W.; Qian, Y.; Lang, S.; Wang, R. The Undisturbed-Soil Experimental Analysis of the Destructive-State Influence of the Plate Diameter under the Vertical Tension on the CEP Pile. *Chem. Eng. Trans.* **2018**, *66*, 445–450.
12. Chen, Y.; Lu, F.; Namdar, A.; Cai, J. Working mechanism of pile group with different pile spacing in dense sand. *Adv. Civ. Eng.* **2019**, *2019*, 5376594. [CrossRef]
13. Fattah, M.Y.; Al-Soudani, W.H.; Omar, M. Estimation of bearing capacity of open-ended model piles in sand. *Arab. J. Geosci.* **2016**, *9*, 242. [CrossRef]
14. Qian, Y.; Chen, X.; Sun, L.; Wang, X.; Chen, Y. Effects of Staggered Plates on the Uplift Failure State and Bearing Capacity of NT-CEP Pile Groups. *Buildings* **2024**, *14*, 719. [CrossRef]
15. Xing, J.; Li, J. The modeling method and the mesh division of the ANSYS. *China Water Transp. (Acad.)* **2006**, *10*, 116–118.
16. Tao, L.; Jie, Z.; Long, X. The influence of modeling methods on the meshing when solid element was used in ANSYS–Taking the design by analysis of dry welding experiment module as an example. *Appl. Mech. Mater.* **2010**, *42*, 235.

17. Jalammanavar, K.; Pujar, N.; Vishnu, R.R. Finite element study on mesh discretization error estimation for ANSYS workbench. In Proceedings of the International Conference on Computational Techniques, Electronics and Mechanical Systems, Belgaum, India, 21–22 December 2018.
18. Tinghai, X.; Guofu, H. Analysis of results and static loading test of squeezed branch pile and boring pile with constant section in soft soil ground. *Geotech. Investig. Surv.* **2010**, *38*, 11–15.
19. Li, Y.H.; Gao, X.J.; Zhong, G.H. Model test and finite element analysis of squeezed and branch pile bared vertical and horizontal loads. *Appl. Mech. Mater.* **2013**, *470*, 1101–1104. [CrossRef]
20. Ouyang, W.; Wan, J.; Liu, S.W.; Li, X. Line-finite-element implementation for driven steel H-piles in layered sands considering post-driving residual stresses. *Adv. Struct. Eng.* **2021**, *24*, 1384–1398. [CrossRef]